CHEMISTRY
A European Journal

Supporting Information

Hyperpolarization of Amino Acids in Water Utilizing Parahydrogen on a Rhodium Nanocatalyst

Lukas Kaltschnee,[a, b] Anil P. Jagtap,[a, b] Jeffrey McCormick,[c] Shawn Wagner,[d] Louis-S. Bouchard,[c] Marcel Utz,[e] Christian Griesinger,[a] and Stefan Glöggler*[a, b]

chem_201902878_sm_miscellaneous_information.pdf

Table of Contents

Abbreviations

Boc	*tert*-butyloxycarbonyl
ESI-HRMS	Electrospray ionization high resolution mass spectrometry
ESOTHERIC	efficient spin order transfer to heteronuclei via relayed INEPT chains
TFA	trifluoroacetic acid
FID	free induction decay
para-H_2	parahydrogen

Synthetic Procedures

General materials and methods

Chemicals were purchased from commercial suppliers and were used without further purification.

All chemicals were purchased from commercial suppliers and used without further purification.

^{1}H, ^{2}H and ^{13}C NMR spectra were recorded on Bruker Avance III HD spectrometers, at 7 T or at 9.4 T. Further details on the instrumentation can be found below in the section "NMR Instrumentation used". The signals of the deuterated solvents were used as internal chemical shift standards. Chemical shifts (δ) were referenced against the solvent residual signals, as reported in ref. [1] [D_2O (4.81 ppm), $CDCl_3$ (7.26 ppm), methanol-d_4 (3.31 ppm)][3]. The chemical shifts in ^{1}H-NMR and ^{13}C-NMR are reported in ppm relative to tetramethylsilane (TMS, δ = 0.00 ppm). All coupling constants were measured in Hertz. All moisture sensitive reactions were carried out in oven-dried glassware using nitrogen industrial grade cylinders. Molecular masses of the labelled materials were determined by ESI-MS (Bruker).

Chemicals

*General procedure 1, used for the preparation of the N-Boc-vinyl Ester of amino acids (**2a,b** and **2a',b'**)*

A mixture of *N*-Boc-amino acid (0.568 mmol), $Pd(OAc)_2$ (0.00567 mmol, 0.01 equiv), KOH (0.0568 mmol, 0.1 equiv) and 0.6 mL of vinyl acetate-d_6 (for unlabeled vinyl acetate:3 mL) was stirred for 24 h at room temperature under N_2. The reaction mixture was filtered on Celite bed and the filtrate obtained was evaporated under reduced pressure. The crude product was purified by flash column chromatography (silica) using a gradient elution (EtOAc: pet ether; 0:100 to 10:90) to give corresponding *N*-Boc-vinyl ester of amino acids (55-65% yield).

*N-Boc vinyl glycine **2a'** (unlabeled compound)*

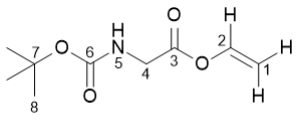

2a'

^{1}H-NMR ($CDCl_3$, 300.13 MHz; 298 K) δ = 7.25 (dd, 1H, $^3J_{HH}$ = 13.9 Hz, $^3J_{HH}$ = 6.1 Hz, 2-H), 4.95 (br s, 1H, 5-H), 4.94 (dd, 1H, $^3J_{HH}$ = 13.9 Hz, $^2J_{HH}$ = 1.8 Hz, 1a-H), 4.63 (dd, 1H, $^3J_{HH}$ = 6.1 Hz, $^2J_{HH}$ = 1.8 Hz, 1b-H), 3.98 (d, 2H, $^3J_{HH}$ = 5.6 Hz, 4-H_2), 1.46 (s, 9H, 8-H_9) ppm.

^{13}C-NMR ($CDCl_3$, 75.47 MHz, 298 K) δ = 167.6 (3-C), 140.8 (2-C), 98.6 (1-C), 80.2 (7-C), 42.3 (4-C), 28.2 (8-C) ppm.

N-Boc vinyl-d_3 glycine-1-$^{13}C_1$ ***2a*** *(labeled compound)*

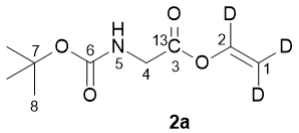

2a

^{1}H-NMR ($CDCl_3$, 300.13 MHz; 320 K) δ = 4.96 (br s, 1H, 5-H), 3.98 (br dd, 2H, 4-H), 1.46 (s, 9H, 8-H) ppm.

^{13}C-NMR ($CDCl_3$, 75.47 MHz, 320 K) δ = 167.6 (3-C), 42.3 (4-C), 28.3 (8-C) ppm.

^{2}H-NMR ($CDCl_3$, 46.07 MHz, 320 K) δ = 4.92 (1a-D), 4.62 (1b-D) ppm.

ESI-HRMS ($^{12}C_8{}^{13}C_1{}^1H_{12}{}^2H_3NO_4$)

positive mode:	calculated: m/z = 228.1115 $[M+Na]^+$	measured: m/z = 228.1116 $[M+Na]^+$
	calculated: m/z = 206.1296 $[M+H]^+$	measured: m/z = 206.1287 $[M+H]^+$
	calculated: m/z = 244.0855 $[M+K]^+$	measured: m/z = 244.0858 $[M+K]^+$

N-Boc vinyl alanine ***2b'*** *(unlabeled compound)*

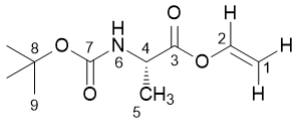

2b'

^{1}H-NMR ($CDCl_3$, 400.13 MHz; 298 K) δ = 7.24 (dd, 1H, $^3J_{HH}$ = 13.9 Hz, $^3J_{HH}$ = 6.2 Hz, 2-H), 4.96 (br s, 1H, 6-H), 4.94 (dd, 1H, $^3J_{HH}$ = 13.8 Hz, $^2J_{HH}$ = 1.8 Hz, 1a-H), 4.63 (dd, 1H, $^3J_{HH}$ = 6.2 Hz, $^2J_{HH}$ = 1.8 Hz, 1b-H), 4.36 (bm, 1H, 4-H), 1.45 (s, 9H, 9-H_9), 1.43 (d, 3H, $^3J_{HH}$ = 7.2 Hz, 5-H_3) ppm.

N-Boc vinyl-d_3 alanine-1-$^{13}C_1$ ***2b*** *(labeled compound)*

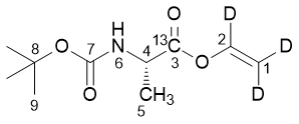

2b

^{1}H-NMR ($CDCl_3$, 300.13 MHz; 320 K) δ = 4.94 (br s, 1H, 6-H), 4.36 (br m, 1H, 4-H), 1.46-1.40 (br m, 12H, 9-H & 5-H) ppm.

^{13}C-NMR ($CDCl_3$, 75.47 MHz, 320 K) δ = 170.5 (3-C), 49.2 (4-C), 28.3 (9-C), 18.2 (5-C) ppm.

^{2}H-NMR ($CDCl_3$, 46.07 MHz, 320 K) δ = 4.92 (1a-D), 4.62 (1b-D) ppm.

ESI-HRMS ($^{12}C_9{}^{13}C_1{}^1H_{14}{}^2H_3NO_4$)

positive mode:	calculated: m/z = 242.1272 $[M+Na]^+$	measured: m/z = 242.1274 $[M+Na]^+$
	calculated: m/z = 220.1452 $[M+H]^+$	measured: m/z = 220.1447 $[M+H]^+$
	calculated: m/z = 258.1011 $[M+K]^+$	measured: m/z = 258.1011 $[M+K]^+$

General procedure 2, used for N-Boc deprotection

The *N*-Boc protected amino acid vinyl esters (**2a**, **2b**, **2a'**, **2b'**) were dissolved in $CDCl_3$ at varying concentrations (c_0 = 70 mM – 120 mM) inside a 5 mm NMR tube. TFA was added to the solutions, to yield a 10%of TFA in $CDCl_3$. The sample was placed inside an NMR spectrometer, heated to 320 K, and the reaction conversion was monitored via ^{1}H-NMR. Upon reaching >95%

conversion (25 – 100 min.), the samples were removed from the magnet, transferred to a round bottom flask, 5 ml methanol were added, and the solvents were removed by rotary evaporation. The addition of 5 ml methanol with subsequent evaporation of the solvent was repeated until the flasks reached a steady weight (five to eight drying steps). The products were stored at -10 °C.

*Preparation of the vinyl glycine **3a'** TFA salt (unlabeled compound)*

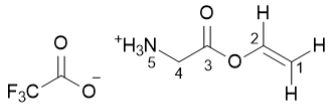

3a'

Preparation from **3a'** was performed, according to general procedure 2. c_0 = 120 mM; reaction duration: 45 min.; yield: quant.

^{1}H-NMR (D_2O 56 mM DCl, 300.13 MHz; 298 K) δ = 7.22 (dd, 1H, $^3J_{HH}$ = 13.8 Hz, $^3J_{HH}$ = 6.2 Hz, 2-H), 5.09 (dd, 1H, $^3J_{HH}$ = 13.8 Hz, $^2J_{HH}$ = 2.1 Hz, 1a-H), 4.84 (dd, 1H, $^3J_{HH}$ = 6.2 Hz, $^2J_{HH}$ = 2.1 Hz, 1b-H), 4.03 (s, 3H, 4-H_2) ppm.

^{13}C-NMR (D_2O 56 mM DCl, 75.47 MHz, 298 K) δ = 165.7 (3-C), 140.4 (2-C), 100.6 (1-C), 39.9 (4-C) ppm.

*Preparation of the vinyl-d_3 glycine-1-$^{13}C_1$ **3a** TFA salt (labeled compound)*

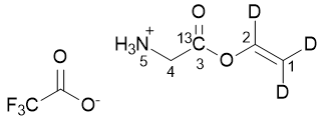

3a

Preparation from **3a** was performed, according to general procedure 2. c_0 = 76 mM; reaction duration: 25 min.; yield: 91%

^{1}H-NMR (D_2O 56 mM DCl, 300.13 MHz; 298 K) δ = 4.02 (d, 2H, $^2J_{CH}$ = 6.7 Hz, 4-H) ppm.

^{13}C-NMR (D_2O 56 mM DCl, 75.47 MHz, 298 K) δ = 165.7 (3-C), 40.0 (4-C) ppm.

^{2}H-NMR (D_2O 56 mM DCl, 46.07 MHz, 298 K) δ = 7.20 (2-D) ppm.

ESI-HRMS ($^{12}C_3{}^{13}C_1{}^1H_5{}^2H_3NO_2^+$)

positive mode: calculated: m/z = 106.0771 $[M]^+$ measured: m/z = 106.0770 $[M]^+$

*Preparation of the vinyl alanine **3b'** TFA salt (unlabeled compound)*

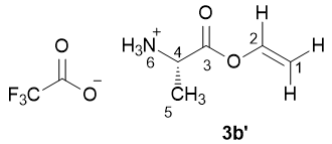

3b'

Preparation from **3b'** was performed, according to general procedure 2. c_0 = 100 mM; reaction duration: 95 min.; yield: quant.

^{1}H-NMR (methanol-d_4, 400.13 MHz; 298 K) δ = 7.32 (dd, 1H, $^3J_{HH}$ = 13.8 Hz, $^3J_{HH}$ = 6.2 Hz, 2-H), 5.07 (dd, 1H, $^3J_{HH}$ = 13.8 Hz, $^2J_{HH}$ = 2.1 Hz, 1a-H), 4.80 (dd, 1H, $^3J_{HH}$ = 6.2 Hz, $^2J_{HH}$ = 2.1 Hz, 1b-H), 4.22 (q, 1H, $^3J_{HH}$ = 7.3 Hz, 4-H), 1.58 (d, 3H, $^3J_{HH}$ = 7.3 Hz, 5-H_3) ppm.

^{13}C-NMR (methanol-d_4, 100.6 MHz, 298 K) δ = 167.1 (3-C), 140.5 (2-C), 98.9 (1-C), 48.2 (4-C), 14.4 (5-C) ppm.

Preparation of the vinyl-d_3 alanine-1-$^{13}C_1$ ***3b*** *TFA salt (labeled compound)*

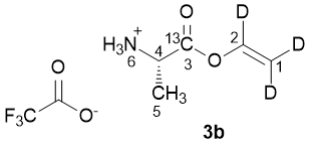

3b

Preparation from **3b** was performed, according to general procedure 2. c_0 = 70 mM; reaction duration: 35 min.; yield: 86%

^{1}H-NMR (methanol-d_4, 300.13 MHz; 298 K) δ = 4.22 (td, 1H, $^3J_{HH}$ = 7.2 Hz, $^2J_{CH}$ = 6.6 Hz, 4-H), 1.59 (dd, 3H, $^3J_{HH}$ = 7.2 Hz, $^3J_{CH}$ = 4.8 Hz, 5-H) ppm.

^{13}C-NMR (methanol-d_4, 75.47 MHz, 298 K) δ = 167.1 (3-C), 140.2 (2-C), 98.3 (1-C), 48.1 (4-C), 14.5 (4-C) ppm.

^{2}H-NMR (methanol-d_4, 46.07 MHz, 298 K) δ = 7.31 (2-D) ppm.

ESI-HRMS ($^{12}C_4{}^{13}C_1{}^1H_7{}^2H_3NO_2^+$)

positive mode: calculated: m/z = 120.0928 $[M]^+$ measured: m/z = 120.0930 $[M]^+$

Preparation of N-acetylcysteine capped Rh-nanoparticle catalyst (NAC@Rh)

The nanoparticle catalyst was prepared, as described in ref. [2]

NMR Instrumentation

All PHIP hyperpolarization experiments were performed on an Avance III HD narrow bore system (Bruker Biospin, Karlsruhe), operating at 7.05 T field strength (^{1}H: 300.13 MHz, ^{13}C: 75.47 MHz, ^{2}H: 46.07 MHz). The system was equipped with a 5 mm double-band direct probe (BBFO-H-D), equipped with a z-gradient. 90° pulses of 9.5 µs, 8 µs and 200 µs were used for^{1}H, ^{13}C and ^{2}H, respectively. A BCU-II chiller (Bruker Biospin, Karlsruhe) was used for temperature regulation. TopSpin 3.5 patchlevel 7 was used for acquisition. For *para*-H_2 experiments, magnetic valves controlling the pressurization and bubbling of the sample are controlled by the spectrometers TTL output signals. For pressurized samples, a backpressure valve constantly keeps the sample pressure at 7 bar. A Bruker parahydrogen generator (BPHG 90) was used to deliver *para*-H_2 enriched hydrogen at pressures above 7 bar. The *para*-H_2 enrichment was experimentally found to be around 80%, as determined by comparing the ^{1}H signal integral of enriched gaseous hydrogen with that of hydrogen that was not enriched, at the same gas pressure (7 bar).

For some of the signal assignment spectra a Bruker Avance III HD spectrometer operating a 9.4 T shielded magnet (^{1}H: 400.13 MHz, ^{13}C: 100.61 MHz, ^{2}H: 61.42 MHz, ^{15}N: 40.54 MHz) was used. The system was equipped with a room temperature 5 mm inverse quadruple resonance probe (QXI-H/P-C/N-D) equipped with a z-gradient. 90° hard pulses used with this probe were 9.75 µs for ^{1}H and 14.1 µs for ^{13}C. A BCU II using was used for temperature regulation.

For the T_1 and T_2 measurements using thermally polarized samples a Bruker Avance NEO spectrometer operating at 14.1 T (^{1}H: 600.25 MHz, ^{13}C: 150.93 MHz) was used. The system was equipped with a cryogenically cooled 5 mm triple resonance inverse probe (TCI-H/F-C/N-D) equipped with a z-gradient. 90° hard pulses used were 8.0 µs for ^{1}H and 12.0 µs for ^{13}C.

PHIP Hyperpolarization experiments

Settings used for all experiments

All ^{1}H-spectra were acquired with a spectral width of 14.0 ppm, collecting 8192 complex data points (1.95 s acquisition). The ^{1}H-transmitter was placed at 5.63 ppm, unless selective proton inversion was used in which case it was set to 2.00 ppm. The spectra were 4x zero-filled and subject to an exponential apodization causing a 0.5 Hz line broadening, prior for Fourier transformation.

^{13}C-spectra used a spectral width of 200.7 ppm with the transmitter placed at 183 ppm. 65536 complex data points (4.33 s acquisition) were used, with the exception of the first acquisition in pulse sequence element E) in Fig. 1 of the main article, for which 16384 complex data points (1.08 s acquisition) were used. The spectra were 4x zero-filled and subject to an exponential apodization causing a 0.5 Hz line broadening, prior for Fourier transformation.

All experiments used for concentration determinations via signal integration were recorded with at receiver gain of 5 for ^{1}H-acquisition and of 10 for ^{13}C-acquisition.

For ^{1}H and ^{2}H heteronuclear broadband decoupling, the WALTZ-16[3] sequence was used with the 90° pulse lengths for decoupling adjusted to 90 µs and 940 µs for ^{1}H and ^{2}H, respectively.

Concentration determination procedure

For concentration determination from ^{1}H spectra, the thermal signals of the H_α protons of glycine-1-^{13}C (T_1 = 8.0 s) or the H_β protons of alanine-1-^{13}C (T_1 = 4.0s), or their respective ethyl-d_3 esters, were integrated. Spectra for concentration determination were collected after performing the PHIP experiments, after a series of pulses and delays (>2 min) which ensure complete hyperpolarization decay. At least eight scans were collected, using 90° excitation and recovery delays of 30 s. The signal intensities were compared to reference spectra collected on a 500 mM maleic acid sample in D_2O and on a 400 mM succinic acid sample in D_2O. The reference molar integrals $I_{m,ref}$ agreed within a margin of ± 4%, for these two samples, which was used as error estimate for the reference. Identical sample filling volumes and acquisition parameters were used for all spectra used for concentration determination, with exception for the number of scans, which varied, and the recovery delay, which was 120 s for the reference spectra. Correct probe matching was ensured for all samples, prior to the acquisition of spectra, used for quantification. All spectra used for signal quantification were checked for correct phasing and then subject to an automated baseline correction procedure. Only signals with sufficient baseline separation from neighboring peaks were used for quantification.

The reference spectra were used to compute reference molar integrals $I_{m,ref}$ according to

$$I_{m,ref} = \frac{I_{ref}}{c_{ref}\eta_{ref}NS_{ref}}. \qquad (S1)$$

Here, I_{ref} is the integral used for referencing, c_{ref} is the reference material concentration, η_k is the number of chemically equivalent nuclei contributing to the reference signal and NS_{ref} is the number of scans acquired in the reference spectrum.

For concentration estimation, thermal signal integrals I_k were converted to concentrations c_k, using

$$c_k = \frac{I_k}{I_{m,ref}\eta_k NS_{therm}}. \qquad (S2)$$

η_k is the number of chemically equivalent nuclei contributing to the thermal signal used and NS_{therm} is the number of scans acquired in the spectrum used for concentration measurement. To estimate errors for these concentrations, the signal-to-noise $\left(S/N\right)_k$ ratio was determined for the target signal, and the error for I_k was estimated as

$$\Delta I_k = \frac{I_k}{\left(S/N\right)_k}. \qquad (S3)$$

The errors for the concentrations were subsequently estimated via error propagation

$$\Delta c_k = \sqrt{\left(\frac{\Delta I_k}{I_{m,ref}\eta_k NS}\right)^2 + \left(-\frac{I_k}{I_{m,ref}^2\eta_k NS}\Delta I_{m,ref}\right)^2}. \quad (S4)$$

Since multiple spectra were measured for the same sample stocks, as described below, the concentrations measured for the same sample stock were combined to yield an average concentration estimate c_{est} for the full stock. Samples which were diluted during the hyperpolarization procedure via the addition of sodium deuteroxide were excluded from this averaging. Error weighed averages were used, as detailed in the following.

Error weighed averaging procedure

All average quantities $\bar{x}$ presented, which were measured from multiple samples were computed using error weighed averaging of the individual quantities x_i according to

$$\bar{x} = \sum_i w_i x_i. \quad (S5)$$

with the weights w_i being proportional to ${\Delta x_i}^{-2}$, with Δx_i being the error estimates for the individual measurement of x_i.

$$w_i = {\Delta x_i}^{-2} \Big/ \sum_k \left[{\Delta x_k}^{-2}\right]. \quad (S6)$$

Since the original estimates of Δx_i may potentially be underestimated, which usually leads to an underestimation of the error for $\bar{x}$, we chose to combine the usual error estimate obtained from error propagation

$$\Delta \bar{x}_{EP} = \sqrt{\sum_i (w_i \Delta x_i)^2} \quad (S7)$$

with the standard deviation $SD(x_i)$ of the individual measurements, via

$$\Delta \bar{x} = \sqrt{\left(SD(x_i)\right)^2 + (\Delta \bar{x}_{EP})^2} \quad (S8)$$

as an error estimate for $\bar{x}$.

Sample preparation and para-H_2 addition

Samples used for PHIP experiments, were prepared at room temperature, with a filling volume of 400 µl. For PHIP-hyperpolarization, 0.5%-w/w DCl (40%-w/w in D_2O) were added to all D_2O stocks, yielding a pH 2 (according to pH paper). Stocks were prepared, containing 0.5 mg/mL NAC@Rh (P260) and ~1 mM of the unprotected amino acids **4a/b**, as the respective TFA salts. Since these salts were found to be hygroscopic, the final stock concentrations were determined as described above, by collecting thermal spectra for all samples after hyperpolarization decay.

Samples were bubbled with N_2, pressurized with 7 bar of N_2-pressure and inserted into the probe, which was preheated to 80°C. All PHIP experiments were performed within a time-frame of 4 - 8 min. after sample insertion. Samples were bubbled with *para*-H_2 (80% enrichment) at 7 bars for 30 s, followed by a delay of 1 s for sample homogenization and the corresponding pulse sequences.

^{1}H-hyperpolarization experiments

For ^{1}H hyperpolarization experiments, a hard 45° ^{1}H pulse was applied, and the FID was detected directly after. The signal integral (magnitude) $I_{PHIP,k}$ was then compared to the normalized average thermal signal $\overline{I_{therm,norm}}$ obtained from the samples of the same stock, to which no sodium deuteroxide was added. To obtain $\overline{I_{therm,norm}}$, the measured thermal signals $I_{therm,k}$ were normalized according to

$$I_{therm,norm,k} = \frac{I_{therm,k}}{\eta_k NS_{therm}}, \quad (S9)$$

with η_k as the number of chemically equivalent nuclei and NS_{therm} as the number of scans, as above, and the corresponding error $\Delta I_{therm,norm,k}$ was estimated from the signal to noise ratio of the peak.

$$\Delta I_{therm,norm,k} = \frac{I_{therm,norm,k}}{(S/N)_k}. \quad (S10)$$

The $\Delta I_{therm,norm,k}$ for one stock were then averaged, as described in equations *(S5)* - *(S8)*, to yield $\overline{I_{therm,norm}}$.

Signal enhancement factors ε_k were then computed according to

$$\varepsilon_k = \frac{I_{PHIP,k}}{\overline{I_{therm,norm}}}, \quad (S11)$$

and the corresponding errors $\Delta\varepsilon_k$ were estimated, as

$$\Delta\varepsilon_k = \sqrt{\left(-\frac{I_{PHIP,k}}{\overline{I_{therm,norm}}^2}\Delta\overline{I_{therm,norm}}\right)^2}. \quad (S12)$$

The integration error for $I_{PHIP,k}$ was found to be insignificant in all cases.

Polarizations *P* were then computed, according to

$$P_k = q\varepsilon_k P_{thermal}, \text{ with } P_{thermal} = \frac{e^{-\frac{1}{2}K} - e^{+\frac{1}{2}K}}{e^{-\frac{1}{2}K} + e^{+\frac{1}{2}K}} \text{ and } K = \frac{\gamma\hbar B_0}{k_B T}, \quad (S13)$$

where $P_{thermal}$ is the thermal polarization expected for an ensemble of identical spin-1/2 nuclei at the given field B_0 and temperature T, $q = 2$ is a factor accounting to the fact, that the 45° pulse used converts only half of the polarization created into observable antiphase signals[4], γ is the gyromagnetic ratio of the nucleus, $\hbar$ is the Planck constant divided by 2π, B_0 is the static magnetic field and k_B is the Boltzmann constant.

The error estimates for the polarizations were obtained from

$$\Delta P_k = q\Delta\varepsilon_k P_{thermal} \quad (S14)$$

and the average polarizations reported, were obtained with the above-described averaging procedure.

^{13}C hyperpolarization

For ^{13}C hyperpolarization experiments, the ESOTHERIC sequences shown in Fig. 1 A) - E) of the main article were used. The delays used were $\Delta_1 = \Delta_3 = 78.1$ ms, $\Delta_2 = 35.2$ ms and $\Delta_4 = 35.2$ ms. Experiments with and without ^1H decoupling during acquisition were recorded. For experiments with addition of sodium deuteroxide addition, the *para*-H_2 overpressure was released after acquisition of the first FID, and 100 µl of 2.5 M sodium deuteroxide was added quickly to the sample, through a tube ending above the solution. The total spacing between the acquisition before and after addition of sodium deuteroxide (NaOD) was 11 s.

The stock concentration estimates obtained c_{est} were used to obtain signal enhancements, by comparing to a ^{13}C reference spectrum collected with a (100 ± 5) mM pyruvate-1-^{13}C sample (> 99% isotope enrichment) in D_2O. The spectrum had been collected with 64 scans and a relaxation delay of 600 s (T_1 = 21.6 s at 80°C in D_2O), after manual 90°-pulse calibration. (*Nota bene*: Fig. 2 of the main text shows a single scan spectrum, for easier comparison.) The molar reference integral $I_{m,ref}$ was computed according to equation *(S1)*.

Enhancement factors for the esters **4a,b** were computed from the observed ^{13}C-siganl integrals $I_{4a/b}$ using

$$\varepsilon_{4a/b} = \frac{I_{4a/b}}{I_{m,ref} c_{est} \sin\theta}, \quad (S15)$$

where θ is the flip angle used for acquisition.

Enhancement factors for the free amino acids **5a,b** were computed, using a factor 5/4 to account for dilution of the samples from 400 µl to 500 µl, according to

$$\varepsilon_{5a/b} = \frac{I_{5a/b}}{I_{m,ref} c_{est} \cos\theta} \frac{5}{4}. \qquad (S16)$$

Errors were estimated from the uncertainty of the stock concentration Δc_{est}, from the error of the reference integral $\Delta I_{m,ref}$ and assuming an integration error according to equation *(S3)*.

$$\varepsilon_{4a/b} = \sqrt{\left(-\frac{I_{4a/b}\Delta c_{est}}{I_{m,ref} c_{est}^2 \sin\theta}\right)^2 + \left(-\frac{I_{4a/b}\Delta I_{m,ref}}{I_{m,ref}^2 c_{est} \sin\theta}\right)^2 + \left(\frac{\Delta I_{4a/b}}{I_{m,ref} c_{est} \sin\theta}\right)^2} \qquad (S17)$$

$$\varepsilon_{5a/b} = \frac{5}{4}\sqrt{\left(-\frac{I_{5a/b}\Delta c_{est}}{I_{m,ref} c_{est}^2 \cos\theta}\right)^2 + \left(-\frac{I_{5a/b}\Delta I_{m,ref}}{I_{m,ref}^2 c_{est} \cos\theta}\right)^2 + \left(\frac{\Delta I_{5a/b}}{I_{m,ref} c_{est} \cos\theta}\right)^2} \qquad (S18)$$

The enhancement factors were then converted into polarizations, according to equations *(S13)* and *(S14)*, using $q = 1$.

Amino acid vinyl ester stability tests in water

Vinyl glycine stability in D_2O, pH 2

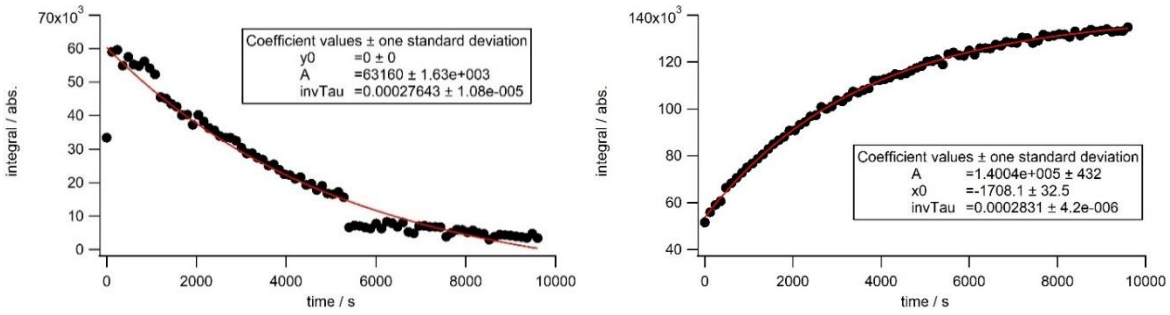

Figure S1: Integral of the H_α protons of vinyl glycine (left) and of its decomposition product (right) during storage at 353 K. A 50 mM sample of **3a'** was prepared in D_2O at pH 2. The data is fit to y(t) = y0 + A*exp(-invTau*t), with y0 fixed to 0, for the left plot. At the start of the measurement series, the sample had already undergone significant decomposition (~ 40%), so the origins of the time axes do not represent the point of initial sample preparation.

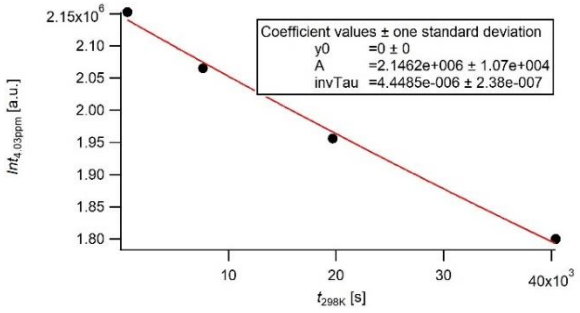

Figure S2: Integral of the H_α protons of vinyl glycine during storage at 298 K. A 50 mM sample of **3a'** was prepared in D_2O at pH 2. The data is fit to y(t) = A*exp(-invTau*t).

298 K (pH 2, no catalyst added)	τ_{dec} = (63 +/- 5) h
353 K (pH 2, no catalyst added)	τ_{dec} = (59 +/- 1) min

Vinyl alanine stability in D_2O, pH 2

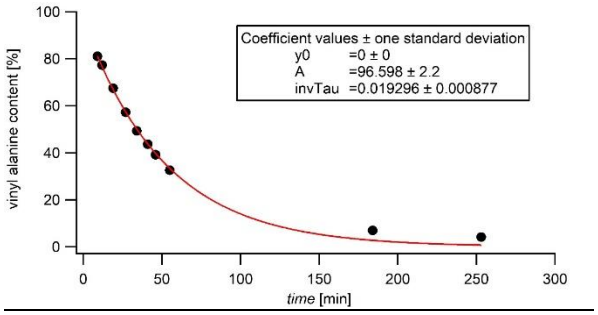

Figure S3: Content of vinyl alanine not decomposed, as judged from integration of the vinyl alanine H_β peaks and the H_β peak of its decomposition product. A 5 mM sample of **3b'** was prepared in D_2O, pH 2, with 0.5mg/mL NAC@Rh. The data is fit to y(t) = A*exp(-invTau*t).

353 K (pH 2, with NAC@Rh)	τ_{dec} = (51.8 +/- 3) min

Antiphase ESOTHERIC – coupling constant determination from ^{13}C hyperpolarized spectra

The measurements $^2J_{CH\alpha}$ and $^3J_{CH\beta}$ couplings in ethyl glycine (**4a**) and ethyl alanine (**4b**) were performed on freshly hyperpolarized samples, to avoid the need for high sample concentrations or long accumulation. To this end, we created ^{1}H spin-order ($I_{1z}I_{2z}$) using PHIP and then used the antiphase ESOTHERIC experiment shown in Figure S4 to produce hyperpolarized ^{13}C signals, from which the unknown couplings can be extracted. For the ethyl-d_3 ester motive used in this work, the sequence can provide close to complete conversion of $I_{1z}I_{2z}$ into $I_{1z}I_{3x}$ (neglecting relaxation), irrespective of the presence of additional "passive" coupling partners to the heteronucleus. The signals detected are antiphase with respect to the $^3J_{CH1}$ coupling, in-phase with respect to all other ^{1}H-^{13}C couplings and free from dispersive contributions, which may hamper coupling constant extraction.

For signals, with well resolved multiplet components, the couplings can directly be extracted from the peak separations within the observed multiplets. The spectra of ethyl-d_3 glycine-1-^{13}C (**4a**) shown in Figure S5 provide a nice example for this. For multiplets experiencing partial cancellation of antiphase multiplet components, as in the case of ethyl-d_3 alanine-1-^{13}C (**4b**), peak shape simulations may be required for reliable coupling constant extraction.

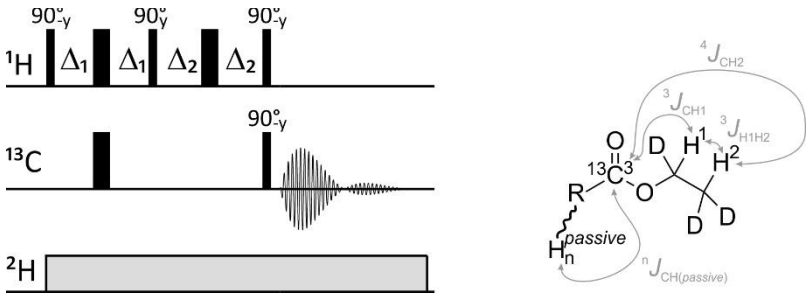

Figure S4: Left: Pulse sequence of the antiphase ESOTHERIC experiment, used for coupling constant extraction. We used $\Delta_1 = 1/(4\ ^3J_{CH1})$ and $\Delta_2 = 1/(4\ ^3J_{H1H2})$. Hard 90° and 180° pulses are represented as narrow and wide bars, respectively. Pulse phases are x, unless otherwise stated. ^{2}H broadband heteronuclear decoupling is indicated with a grey bar. Right: Exemplary spin system, to which the antiphase ESOTHERIC experiment can be applied for coupling constant measurement.

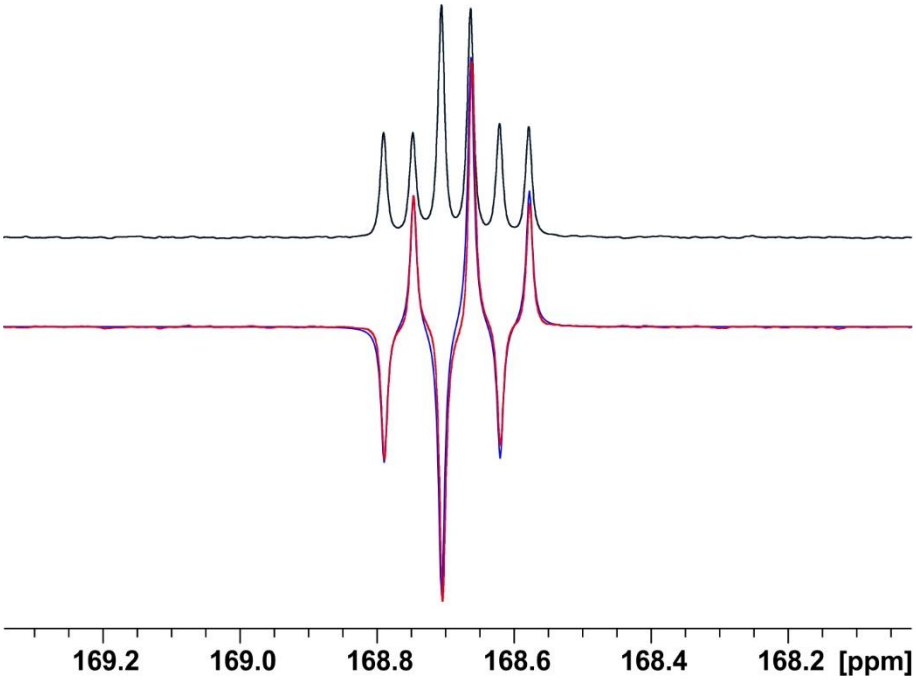

Figure S5: ^{13}C signal of hyperpolarized **4a**. Red: Signal acquired with antiphase ESOTHERIC experiment (Figure S4). Black: Signal acquired with the unmodified ESOTHERIC experiment (elements A+B in Figure 1 of the main article). Blue: Simulated spectrum using the spin system definitions given in Table S3 (see below), starting from $I_{1z}I_{2z}$ spin order and evolving it through the antiphase ESOTHERIC experiment. An FID with a dwell time of 1.056 ms and 4096 data points was simulated. Further details on the simulation are provided below (page S15). Spectra plotted with 0.5 Hz linebroadening.

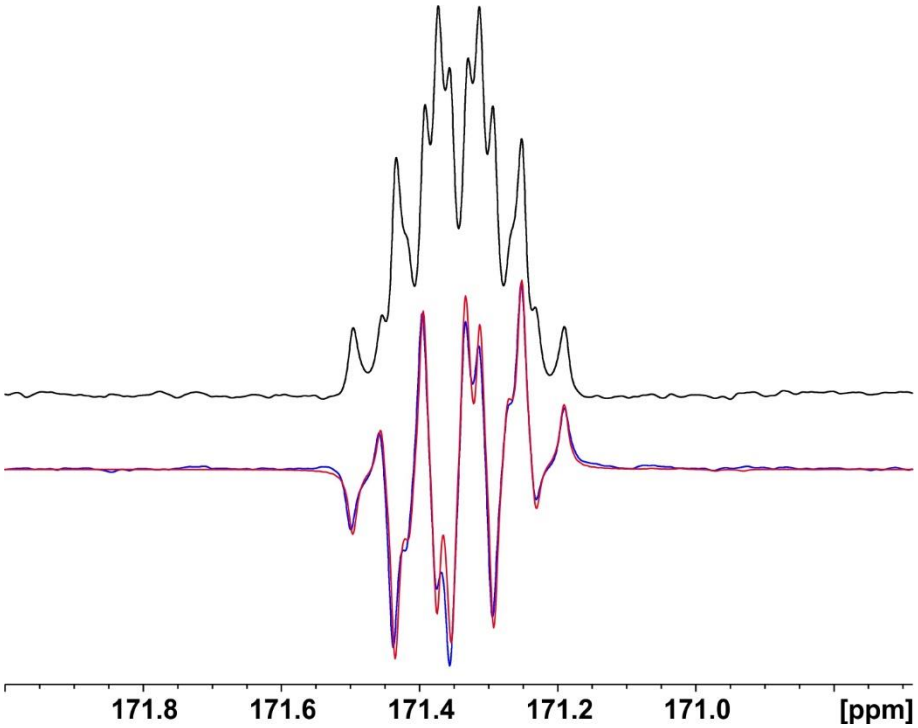

Figure S6: ^{13}C signal of hyperpolarized **4b**. Red: Signal acquired with antiphase ESOTHERIC experiment (Figure S4). Black: Signal acquired with selectively decoupled ESOTHERIC experiment (elements A+C in Figure 1 of the main article). Blue: Simulated spectrum using the spin system definitions given in Table S4 (see below), starting from $I_{1z}I_{2z}$ spin order and evolving it through the antiphase ESOTHERIC experiment. An FID with a dwell time of 10 ms and 128 data points was simulated. Further details on the simulation are provided below (page S15). Spectra plotted with 1.0 Hz linebroadening.

Detailed results of the hyperpolarization experiments

Table S1: Full table of ^{1}H and ^{13}C polarization data for glycine-1-^{13}C (**5a**) and for glycine-1-^{13}C ethyl-1,2,2-d_3 ester (**4a**)

		stock concentration estimate					hyperpolarization yield							
	Sample #	Int. thermal (β-H_3) [a.u.]	NS	S/N	c [mM]	c_{est} [mM]	θ [°]	Int. hyperpol. [a.u.]	ε(^{1}H, **4a**, CHD_2)	*P*(^{1}H, **4a**, CHD_2) [%]	ε(^{13}C, **4a**)	*P*(^{13}C, **4a**) [%]	ε(^{13}C, **5a**)	*P*(^{13}C, **5a**) [%]
stock 1	31	12900	8	20.2	0.64 ± 0.05	0.70 ± 0.07	45	274400	290 ± 30	1.20 ± 0.11				
	33	13700	8	17.2	0.67 ± 0.05		45	271600	290 ± 30	1.19 ± 0.10				
	34	14100	8	16	0.70 ± 0.06		45	278900	300 ± 30	1.22 ±0.11				
		126100	64	47.7	0.78 ± 0.04									
stock 2	60	12400	8	13.4	0.61 ± 0.06	0.63 ±0.07	45	219500	280 ± 30	1.13 ± 0.11				
	61	12200	8	14.4	0.60 ± 0.05		45	226000	280 ± 30	1.16 ± 0.12				
	62	13800	8	14.5	0.68 ± 0.06		45	205900	260 ± 30	1.06 ± 0.11				
	63	10900	8	12.3	0.54 ±0.05		90	1737000			1800 ± 200	0.91 ±0.11		
	64	14590	8	15.6	0.72 ±0.06		90	1771000			1800 ± 200	0.93 ± 0.11		
	65	13950	8	11.9	0.69 ± 0.07		90	1805000			1900 ± 300	0.95 ± 0.11		
		202100	128	48.0	0.62 ± 0.03									
	66	13600	8	13.5	0.67 ± 0.06		90	1659000			1700 ± 200	0.87 ± 0.10		
stock 3	72	13300	8	13.4	0.66 ± 0.06	0.70 ± 0.08								
	73	15900	8	13.0	0.78 ± 0.07		45	235700	270 ± 30	1.08 ± 0.12				
	74	14000	8	13.3	0.69 ± 0.06		45	231300	260 ± 30	1.06 ± 0.11				
	75						1.8	50000; 597000			1500 ± 300	0.75 ± 0.13	690 ± 90	0.35 ± 0.05
	76						1.8	37000; 562000			1100 ± 200	0.56 ± 0.10	650 ± 80	0.33 ± 0.04
	77						18	462000; 430000			1400 ± 200	0.71 ± 0.09	520 ± 70	0.27 ± 0.04
	78						18	421000; 421000			1300 ± 200	0.65 ± 0.08	510 ± 60	0.26 ± 0.04
average										1.14 ± 0.08		0.8 ± 0.2		0.29 ±0.05

Table S2: Full table of ^{1}H and ^{13}C polarization data for alanine-1-^{13}C (**5b**) and for alaine-1-^{13}C ethyl-1,2,2-d_3 ester (**4b**)

		stock concentration estimate					hyperpolarization yield							
	Sample #	Int. thermal (β-H_3) [a.u.]	NS	S/N	c [mM]	c_{est} [mM]	θ [°]	Int. hyperpol. [a.u.]	ε(^{1}H, **4b**, CHD_2)	P(^{1}H, **4b**, CHD_2) [%]	ε(^{13}C, **4b**)	P(^{13}C, **4b**) [%]	ε(^{13}C, **5b**)	P(^{13}C, **5b**) [%]
stock 1	37	29300	8	15.6	0.96 ± 0.08	0.91 ± 0.06	45	282500	240 ± 20	1.00 ± 0.06				
	38	28500	8	14.9	0.94 ± 0.08		45	282500	240 ± 20	1.00 ± 0.06				
	39	25500	8	14.0	0.84 ± 0.07		45	303800	260 ± 20	1.07 ±0.06				
		223200	64	40.1	0.92 ± 0.05									
	40	27300	8	14.8	0.90 ± 0.08		45	272900	240 ± 20	0.96 ±0.06				
stock 2	82	22100	8	12.3	0.73 ± 0.07	0.80 ±0.05	45	236800	230 ± 20	0.93 ± 0.06				
	83	23700	8	12.4	0.78 ± 0.08		45	277300	270 ± 20	1.09 ± 0.06				
	84	23100	8	12.5	0.76 ± 0.07		45	286300	280 ± 20	1.13 ± 0.06				
		407900	128	43.7	0.84 ± 0.04									
	85	24400	8	13.1	0.80 ±0.07		90	1960000			1590 ±130	0.82 ± 0.07		
	87						18	526500; 512000			1350 ± 120	0.71 ± 0.06	550 ± 40	0.28 ± 0.02
	88						18	466100; 476000			1230 ± 90	0.63 ± 0.05	510 ± 40	0.26 ± 0.02
	89						18	408100; 404000			1070 ± 100	0.55 ± 0.05	430 ± 30	0.22 ± 0.02
average							18			1.02 ± 0.08		0.65 ± 0.12		0.25 ± 0.04

Spin-dynamics simulations for transfer efficiency estimation in the modified ESOTHERIC experiment

Settings used

Spin-system simulations were performed with SpinDynamica[5] 3.0.2.2, to test the spin-order transfer efficiencies that can be obtained with the ESOTHERIC sequences used (Fig. 1 of the main article, A+B or A+C), in the presence of H_α and H_β protons. Simulations for ethyl-d_3 glycine-1-^{13}C (**4a**) were performed using a 5 spin-1/2 basis and simulations for ethyl-d_3 alanine-1-^{13}C (**4b**) were performed using a 7 spin-1/2 basis. Chemical shifts and couplings were used, as extracted from spectra collected at 80°C in D_2O, which were used for hyperpolarization experiments. The spin systems used are summarized in **Table S3** and **Table S4**. For simplicity, hard 90° pulses on both channels were simulated with 10µs @ γB_1 = 25 kHz. Sections A, B and C of the pulse sequence shown in Fig. 1 of the main article were implemented, as used on the spectrometer, with the exception, that the selective pulse (Rsnob, 8 ms, $\gamma B_{1,max}$ = (2*8ms*0.21589)$^{-1}$) was digitized with 32 discrete amplitude levels, instead of 1000, as used in the experiments. Further, the constants O_{1p} = 165 ppm, O_{2p} = 2.0 ppm, γ_H = 2.67513*10^8 rad T^{-1} s^{-1}, γ_C = 6.72828*10^7 rad T^{-1} s^{-1}, B_0 = 7.04927 T, Δ_1 = (4*3.2 Hz)$^{-1}$ and Δ_2 = (4*7.1 Hz)$^{-1}$ were defined. The time-invariant part of the rotating frame Hamiltonian was defined, as

$$\mathcal{H}_{offs} = -B_0 10^{-6}\left(\gamma_3(\delta_3 - O_{1P})I_{3z} + \sum_{i\neq 3}(\gamma_i(\delta_i - O_{2P})I_{iz})\right) + 2\pi\left(\sum_{k\neq 3} J_{k3}I_{k,z}I_{3,z} + \sum_{k,l\neq 3} J_{kl}I_kI_l\right). \qquad (S19)$$

In all simulation, no relaxation effects were considered, pulses were considered to be perfectly calibrated and perfect sample & rf field homogeneity was assumed.

Table S3: ethyl-d_3 glycine-1-^{13}C spin system used.

#		δ [ppm]	*J* couplings [Hz]
1	methyl ^{1}H	1.749	J_{12} = 7.1
2	methylene ^{1}H	4.790	J_{12} = 7.1; J_{23} = 3.22
3	^{13}C	168.7	J_{23} = 3.22; J_{34} = J_{35} = 6.4
4	$H_{\alpha,1}$	4.328	J_{34} = 6.4
5	$H_{\alpha,2}$	4.328	J_{35} = 6.4

Table S4: ethyl-d_3 alanine-1-^{13}C spin system used.

#		δ [ppm]	*J* couplings [Hz]
1	methyl ^{1}H	1.754	J_{12} = 7.1
2	methylene ^{1}H	4.806	J_{12} = 7.1; J_{23} = 3.22
3	^{13}C	171.35	J_{23} = 3.22; J_{34} = 6.4; J_{35} = J_{36} = J_{37} = 4.6
4	$H_{\alpha,1}$	4.560	J_{34} = 6.4; J_{45} = J_{46} = J_{47} = 7.1
5	$H_{\beta,1}$	2.025	J_{35} = 4.6; J_{45} = 7.1
6	$H_{\beta,2}$	2.025	J_{36} = 4.6; J_{46} = 7.1
7	$H_{\beta,3}$	2.025	J_{37} = 4.6; J_{47} = 7.1

Results

As can be expected from product operator analysis, the polarization transfer efficiency in section A of the sequence is not influenced by the presence of the H_α and H_β protons. Conversion efficiencies from $I_{1z}I_{2z}$ to $-I_{3x}I_{2z}$ were > 99.5% for **4a** and **4b**.

For ethyl-d_3 glycine-1-^{13}C (**4a**), the simulations further confirm, that with Δ_3 = (4*3.2 Hz)$^{-1}$ section B provides conversion from $-I_{3x}I_{2z}$ to $I_{3y}/2$ with >99.9%, under the idealized conditions assumed (see **Figure S7**). This is a direct consequence of $J_{34} \approx 2*J_{23}$. It can be noted at this point, that the conversion efficiency of section B) while neglecting relaxation is given by

$$y_{idealized}(\Delta_3) = \sin(\pi J_{23} 2\Delta_3) \prod_{i \neq 2} \cos(\pi J_{i3} 2\Delta_3). \qquad (S20)$$

When analyzing the ethyl-d_3 glycine-1-^{13}C spin system according to this formula using $\Delta_3 = 1/(4J_{23}) = 78ms$, one obtains

$$y_{Gly}\left(\frac{1}{4J_{23}}\right) = \sin\left(\frac{\pi}{2}\right)\cos\left(\frac{\pi}{2}\frac{J_{34}}{J_{23}}\right)\cos\left(\frac{\pi}{2}\frac{J_{35}}{J_{23}}\right) \approx 1 \cdot (-1) \cdot (-1). \qquad (S21)$$

Evolution under the $^2J_{CH\alpha}$ coupling is fully refocused with these settings, and thus does not hamper polarization transfer efficiency.

The situation is different for the ethyl-d_3 alanine-1-^{13}C spin system. Simply using $\Delta_3 = 1/(4J_{23}) = 78ms$ here leads to

$$y_{Ala}\left(\frac{1}{4J_{23}}\right) = \sin\left(\frac{\pi}{2}\right)\cos\left(\frac{\pi}{2}\frac{J_{34}}{J_{23}}\right)\left(\cos\left(\frac{\pi}{2}\frac{J_{35}}{J_{23}}\right)\right)^3 \approx 1 \cdot (-1) \cdot (-0.623)^3 \approx 0.24. \qquad (S22)$$

It can thus be estimated, that only 24% -$I_{3x}I_{2z}$ to $I_{3y}/2$ conversion efficiency is expected for ethyl-d_3 alanine-1-^{13}C (**4b**) spin system. Whereas the presence to H_α merely changes the magnetization phase, polarization is lost into anti-phase coherences with the H_β-protons, if no active H_β-decoupling ist used. Higher, efficiencies of 57% and 85% are found at Δ_3 = 95 ms and Δ_3 = 225 ms (still neglecting relaxation). These results agree with the simulated results for ethyl-d_3 alanine-1-^{13}C (**4b**), when using element B) for refocusing (see blue trace in **Figure S8**). The simulation for element C) in contrast shows that close to optimal transfer at $\Delta_4 = 1/(8J_{23}) - \delta = 39ms$ can be restored, when selectively inverting the H_β protons during refocusing (see red trace in **Figure S8**). Under the idealized conditions described, >99.5% transfer efficiency is obtained in the simulations at this time point. For Δ_4 = 35.2 ms, which we accidentally used instead of the optimal Δ_4 = 39 ms, still a transfer efficiency of >93% is obtained.

It should be emphasized, that in experiments, the observed transfer efficiencies will be lower, due to non-negligible relaxation, rf-inhomogeneities and other factors.

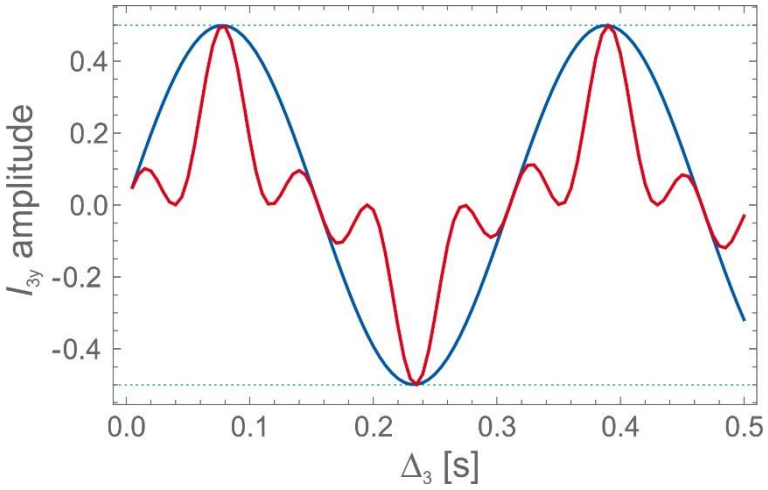

Figure S7: Simulated amplitudes of the I_{3y} coherence after evolving -$I_{3x}I_{2z}$ through evolution block B). Red: Full ethyl-d_3 glycine-1-^{13}C spin system, blue: spin system with the H_α protons removed. The green dotted lines indicate ±100% conversion.

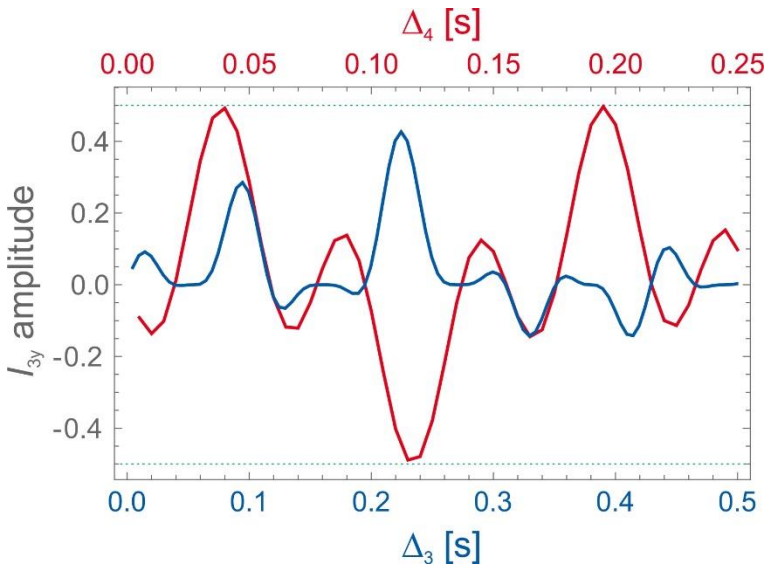

Figure S8: Simulated amplitudes of the I_{3y} yield with start from pure $-I_{3x}I_{2z}$ coherence, in the ethyl-d_3 alanine-1-^{13}C spin system. Blue: evolution through evolution block B), red evolution through evolution block C), using selective decoupling of the H_β position with an 8 ms Rsnob pulse. The two horizontal axes are aligned to yield identical lengths for the overall evolution element ($\Delta_3 = 2\Delta_4$).

Estimate of the relaxation loss during ESOTHERIC for ethyl-d_3 glycine-1-^{13}C (4a)

The preceding analysis neglects possible signal loss caused by relaxation during the ESOTHERIC experiments used, amongst the many factors that can contribute to signal loss during the experiment.

Whereas the transfer efficiencies under idealized conditions that we estimated in the previous section are close to unit for optimal timing settings, in practice we find polarization transfer efficiencies of (70 ± 20)% for ethyl-d_3 glycine-1-^{13}C (**4a**) and (60 ± 20)% for ethyl-d_3 alanine-1-^{13}C (**4b**). Polarization loss induced by relaxation, rf-inhomogeneity, mass transport in- and out of the coil region during the pulse sequence and other factors can therefore not be neglected.

Accurate estimation of these losses would require knowledge of the relaxation parameters of all coherences involved in the coherent magnetization transfer process and therefore is quite challenging. To obtain a rough idea of the relaxation contribution, we herein compare nuclear T_2 values, with the overall length of the ESOTHERIC pulse sequences utilized.

T_2-values were measured exemplarily for a 10 mM sample of ethyl-d_3 glycine-1-^{13}C (**4a**) with 1 mg/mL of the nanoparticle catalyst (NAC@Rh P260) in D_2O. The sample was extensively bubbled with N_2 and subsequently with H_2, before measurement. Measurements were performed at 14 T and 298 K using the thermally polarized compound. The ^{13}C-T_2 value was measured using CPMG[6] with ^{1}H broadband decoupling during acquisition. The ^{1}H-T_2 values were measured using the PROJECT[7] modification to CPMG. This avoids the need for very fast pulsing during CPMG for the coupled spin-system present, at the cost that an averaged apparent T_2 for both nuclei. In addition to these T_2 values,

Table **S5** lists T_1 values measured for the same sample.

Table S5: T_1 and T_2-values measured for ethyl-d_3 glycine-1-^{13}C at 14 T and 289 K.

#		T_1 [s]	T_2 [s]
1	methyl ^{1}H	13.3 ± 1.2	6.4 ± 0.2
2	methylene ^{1}H	20.0 ± 0.2	6.9 ± 0.2
3	^{13}C	13.9 ± 1.1	3.2 ± 0.3
4	$H_{\alpha,1}$	3.4 ± 0.1	2.0 ± 0.1

The ESOTHERIC pulse sequences we used had a total length of roughly 400 ms, prior to storage as ^{13}C z-magnetization (according to Figure 1E of the main article) or signal acquisition (according to Figure 1D of the main article).

During the initial part of the experiment (Figure 1A), which herein was 226 ms long, ^{1}H coherences are transverse. We thus assume that the ^{1}H-T_2 of H^1 and H^2 are determining relaxation-induced signal loss. When assuming a simple exponential decay, the estimated signal loss during this period is ~4%.

During the refocusing periods of the experiment (Figure 1B or 1C), which were ~150 ms long, ^{13}C coherences are transverse, and thus we assume that the ^{13}C-T_2 is determining relaxation. For this period, a ~5% signal loss can thus be estimated.

Under the very simplifying conditions we performed this estimate, a ~10% signal loss is expected during the coherent ESOTHERIC polarization transfer.

Literature

1. G. R. Fulmer, A. J. M. Miller, N. H. Sherden, H. E. Gottlieb, A. Nudelman, B. M. Stoltz, J. E. Bercaw and K. I. Goldberg, *Organometallics*, 2010, **29**, 2176-2179.
2. J. McCormick, S. Korchak, S. Mamone, Y. N. Ertas, Z. Liu, L. Verlinsky, S. Wagner, S. Gloggler and L. S. Bouchard, *Angew Chem Int Ed*, 2018, **57**, 10692-10696.
3. A. J. Shaka, J. Keeler and R. Freeman, *Journal of Magnetic Resonance (1969)*, 1983, **53**, 313-340.
4. R. A. Green, R. W. Adams, S. B. Duckett, R. E. Mewis, D. C. Williamson and G. G. R. Green, *Progress in Nuclear Magnetic Resonance Spectroscopy*, 2012, **67**, 1-48.
5. C. Bengs and M. H. Levitt, *Magnetic Resonance in Chemistry*, 2018, **56**, 374-414.
6. S. Meiboom and D. Gill, *Review of Scientific Instruments*, 1958, **29**, 688-691.
7. J. A. Aguilar, M. Nilsson, G. Bodenhausen and G. A. Morris, *Chemical Communications*, 2012, **48**, 811-813.